Article

Quantification of differential response of tumour and normal cells to microbeam radiation in the absence of FLASH effects

Harriet Steel [1]*[ORCID], **Sarah C. Brüningk** [2,3], **Carol Box**[1], **Uwe Oelfke**[1], and **Stefan H. Bartzsch** [4,]

1   Division of Radiotherapy and Imaging, The Institute Of Cancer Research, 123 Old Brompton Road, London SW7 3RP, United Kingdom; harriet.steel@icr.ac.uk

2   Machine Learning & Computational Biology, Department of Biosystems Science and Engineering, ETH Zurich, Basel, Switzerland

3   Swiss Institute for Bioinformatics (SIB), Lausanne, Switzerland

4   Department of Radiation Oncology, Klinikum rechts der Isar, Technical University of Munich, Ismaninger Straße 22, 81675 Munich, Germany; stefan.bartzsch@tum.de

*   Correspondence: harriet.steel@icr.ac.uk)

1   **Abstract:**

2   Microbeam radiotherapy (MRT) is a pre-clinical method of delivering spatially-fractionated ra-

3   diotherapy aiming to improve the therapeutic window between normal tissue complication and

4   tumour control. Previously, MRT was limited to ultra-high dose rate synchrotron facilities. Here,

5   we investigate *in vitro* effects of MRT at conventional dose rates on tumour and normal cells.

6   Using a bench-top X-ray source four normal and tumour cell lines were exposed to homogeneous

7   broad beam (BB) radiation, MRT, or were separately irradiated with peak or valley doses before

8   being mixed. Clonogenic survival was assessed and compared to BB-estimated surviving fractions

9   calculated by the linear-quadratic (LQ) model. All cell lines showed similar BB sensitivity. BB

10   LQ-model predictions exceeded the survival of cell lines following MRT or mixed beam irradiation.

11   This effect was stronger in tumour compared to normal cell lines. Dose mixing experiments could

12   reproduce MRT survival. We observed a differential response of tumour and normal cells to

13   spatially fractionated irradiations *in vitro* indicating increased tumour cell sensitivity. Importantly,

14   this was observed at dose rates precluding the presence of FLASH effects. The LQ-model did

15   not predict cell survival when the cell population received split irradiation doses indicating that

16   factors other than local dose influenced survival after irradiation.

17   **Keywords:** microbeam; in vitro; compact source; clonogenic survival; integral dose; LQ model;

18   spatial fractionation

Publisher's Note: MDPI stays neutral with regard to jurisdictional claims in published maps and institutional affiliations.

1. Introduction

19

20   Any cancer treatment aims to eradicate the tumour target, whilst inflicting minimal

21 toxicity in healthy tissues. In radiation therapy (RT) this aim is conventionally achieved

22 by geometrically confining the high dose field to the tumour, e.g. by intensity modulated

23 RT, and thereby limiting side effects to organs at risk (OAR). However, exposure of

24 OARs located in close proximity to the tumour, or along the beam path, is inevitable

25 and limits the dose escalation to the tumour with potential implications on outcome.

26 Spatially fractionated RT, such as microbeam radiation therapy (MRT) [1], has previously

27 been suggested as an alternative strategy to maximize the therapeutic window between

28 tumour control and normal tissue complication probability. MRT uses arrays of planar,

29 high-dose beams of tens of μm width which are separated by a few hundred micrometers.

30 This spatial fractionation results in small regions of tissue receiving large (generally

31 300-800 Gy) peak doses being ablated, whereas spared areas receive a several fold lower

32 (valley) dose. In order to maintain the collimated dose pattern, keV photon beams are

33 employed for MRT delivery typically produced at large 3rd generation synchrotrons to

34 prevent motion blurring of the spatial dose pattern through high photon flux delivery.

Pre-clinical *in vivo* data has demonstrated a remarkable normal tissue sparing following MRT, despite peak doses in the range of hundreds of gray [2–8]. It has also been shown that MRT is effective for the treatment of tumours in preclinical models of brain cancer [9–13] and melanoma [14]. Together, these studies suggest that MRT has a differential effect on normal and tumour tissues, indicating its high therapeutic potential for cancer treatment. Currently, the origin of the differential effect of MRT on tumour and normal tissue (referred to as 'the microbeam effect') is a matter of scientific debate. Hypotheses proposed include a role for vascular maturity [15–17], the immune system [18–21] and bystander effects [22,23]. More recently, however, there is growing evidence for normal tissue sparing through the use of ultra-high dose rates delivered at synchrotron facilities (FLASH) [24,25]. Hence, it remains to be seen how much of the normal tissue sparing previously attributed to MRT, is indeed a result of spatial dose fractionation as opposed to FLASH effects.

Moreover, there is little data to support the existence of the microbeam effect *in vitro* [23, 26,27], i.e. in the absence of immune system- or vascular-mediated effects. A differential response to MRT in normal and tumour cells *in vitro* would indicate a role for additional components, such as bystander signalling. Previous work on MRT evaluation *in vitro* either lacked a detailed comparison of normal and tumour cells [26,28], or did not evaluate MRT in relation to conventional BB irradiation. A possible reason may be difficulties in comparing the highly heterogeneous dose profiles of MRT to BB for this purpose. In light of the linear-quadratic relation of cell survival with radiation dose, it is clear that neither mean, peak nor valley dose alone are sufficient for a comparison with BB treatments.

In this study we evaluate the response of four tumour and non-tumour human cell lines in response to BB and MRT to investigate and quantify differential effects of these treatments delivered with a conventional X-ray tube and optional MRT collimation [29]. As such, our system precludes the presence of FLASH effects implying that any differential would exclusively be attributed to spatial fractionation. Moreover, by means of calculating cell survival using BB linear quadratic model parameters and the MRT dose distribution we are able to draw a direct comparison between BB and MRT treatment efficacies.

2. Materials and Methods

2.1. Cell Culture

Human umbilical vein endothelial cells (HUVEC) from pooled donors were purchased from Lonza (Slough, UK) and MRC-5 normal lung fibroblasts, from Sigma Aldrich Ltd. (Germany). For the purposes of this manuscript we will refer to these as "normal" cells. The human non-small cell lung cancer lines A549 and NCI-H23 were obtained from The American Type Culture Collection (ATCC, Gaithersburg, USA). Tumour cell lines were cultured in Dulbecco's minimal essential medium F12 (Gibco Life Technologies Ltd., Paisley, UK), and MRC-5 cells were cultured in minimal essential medium (MEM; Gibco Life Technologies Ltd), both supplemented with 10% foetal bovine serum (PAN Biotech GmbH, Aidenbach, Germany). HUVECs were cultured in endothelial cell growth medium-2 (Lonza) including all supplements supplied by the manufacturer. Cells were maintained in a humidified incubator at $37^\circ C$ and 5% CO2. Screening for mycoplasma contamination was performed by polymerase chain reaction (Surrey Diagnostics, Cranleigh, UK) and cell lines were authenticated in-house by short tandem repeat analysis using a Gene Print 10.0 kit (Promega, Madison, USA) and a 3730xl DNA analyser (Applied Biosystems, Warrington, UK).

2.2. Clonogenic Assay

To ensure that all clonogenic assays were carried out on exponentially growing cells, cells were seeded at approximately 16 hours prior to RT, yielding 80% confluence at time of irradiation. Following irradiation cells were immediately harvested by trypsinisation,

counted and plated at appropriate numbers in triplicate in 6-well plates. Cells were then incubated under the specified culture conditions and allowed to form colonies for 7-14 days, depending on the cell line. Colonies were fixed in ice-cold methanol at -20°C for 20 minutes, left to dry, and stained in 0.5% crystal violet solution (Sigma Aldrich Ltd.). Colonies containing 50 or more cells were counted. Plating efficiency of the cells for each condition was calculated as the ratio of colonies counted per cell number seeded. The clonogenic survival was calculated as the ratio between plating efficiencies of treated and untreated cells. For each experiment three independent repeats were performed and mean values and standard deviations are reported.

2.3. Irradiation procedure

For all experiments X-rays were generated from an X-ray tube (HPZ-160-11, Varian Medical Systems) mounted in an X-ray cabinet (Xstrahl, Camberley, UK). An acceleration voltage of 160 kV, and a tube current of 11.3 mA for BB or 5.6 mA for MRT generation was used. The beam was hardened by 1 mm aluminium filtration resulting in a dose-rate of 0.031 ± 0.002 Gy/s at the sample position for BB exposures. MRT was generated as previously described [29]. In short, a bespoke collimator was mounted 70 mm from the source of the beam. The collimator consisted of 50 μm wide beam-slits spaced 400 μm apart.
The MRT field was characterised following previously published procedure [30] using EBT-XD films (Gafchromic, Bridgewater, US; dynamic dose range of 0.1-60 Gy, spatial resolution of < 25 μm). For absolute dose measurements, calibration films were exposed to 0–100 Gy under BB conditions and correlated with ionisation chamber (Semiflex, PTW, Germany) measurements. Films were also exposed to MRT in cell treatment geometry, i.e. accounting for equal depths of scatter material, here poly(methyl methacrylate), and air gaps. All exposed films were scanned 48 h after irradiation at 4 μm resolution with an optical microscope (Axio Scan, Zeiss, Oberkochen, Germany). Images were corrected for illumination and stitching artefacts using ZEN software (Zeiss, 2011). The dose distribution was measured in three independent experiments for MRT exposure duration between 3.5 and 12 min per film, to cover both peaks and valleys within the dynamic range of the films. For each film a dose rate volume histogram (DVH) was calculated and a mean DVH was generated from three independent repeat measurements (see Figure 1). For each DVH bin, only pixels within the dynamic range of the film were included. The specifications of our system resulted in a heel effect across the exposed area leading to a spread of the individual peak and valley doses and deviation of the DVH for a perfect two peak distribution. Hence, all following data are reported as a function of this full spectrum of doses with errorbars representing the standard deviation over repeat measurements.
For comparison with BB irradiation at two distinct dose levels, the DVH was approximated by a step function resulting in the same integral dose as the MRT dose distribution (see Figure 1, dashed line). The coefficient of determination measured on a log scale between idealized and experimentally measured DVH was $R^2 = 0.85$ which corresponded to a PVDR of 22, and a spatial fraction of 80%/20% of cells receiving the valley/peak dose. This distribution was delivered for dose mixing experiments.

2.4. Dose mixing

Cells were irradiated separately under BB conditions with either a peak or a valley dose, accounting for a constant PVDR of 22. Due to longer exposure duration for MRT experiments, flasks were left at room temperature after irradiation for equivalent amounts of time prior to trypsinisation. Following dissociation and counting, the cells were mixed such that 20% received the peak dose and 80% the valley dose, mimicking the results obtained from the dose rate volume histogram in Figure 1. Cell suspensions were plated for clonogenic survival, as described above.
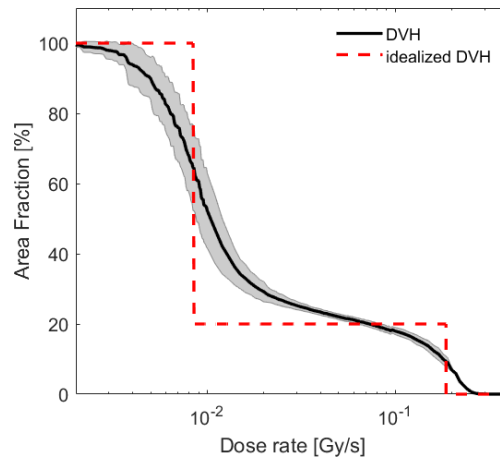
Figure 1. Dose rate volume histogram obtained as an average over 17 film measurements at different exposure duration (solid line). Shaded background corresponds to the standard deviation of these measurements per DVH bin. The dose distribution was approximated by an idealized, two-step DVH (dashed line) corresponding to the same integral dose rate of 0.044 Gy/s, a PVDR of 22 and a fraction of 80/20 % of cells receiving the valley/peak dose.

2.5. Cell survival analysis

The dependence of clonogenic cell survival S on a single fraction of radiation dose d is conventionally described by the linear quadratic (LQ) model [31].

$$S(d) = e^{-Y} = e^{-(\alpha d + \beta d^2)} \tag{1}$$

Here, the biological effect, Y, characterises cell survival as a second order polynomial of the dose d and the cell line and radiation quality dependent parameters α and β. For MRT a fraction $\nu(d_i)$ of the cell culture is exposed to dose d_i, within the spectrum $\{d_i\}$ of N different doses $d_i(i = 1...N)$. Assuming that cells are homogeneously plated this is equal to the area fraction exposed to d_i. The LQ-model predicted survival fraction S_{pred} is then calculated as follows:

$$S_{pred}(\nu(\{d_i\})) = \sum_i^N \nu(d_i) \cdot S(d_i) \tag{2}$$

The clonogenic survival in response to BB irradiation was fitted to the LQ-model in MATLAB (version 2017a) using a nonlinear least square approach resulting in α and β values for each cell line. For MRT and mixing experiments cell survival was predicted according to equation (2) using the α and β values calculated from the BB survival. Statistical analysis was performed by two-way ANOVA testing in SPSS (version 26).

3. Results

In order to compare the effectiveness of BB irradiation relative to MRT we first established the sensitivity of the cell lines to standard BB radiation (Figure 2, Table I). We observed that HUVECs (normal endothelial cells) were the most radiosensitive cells and A549 lung cancer cells were the most radioresistant. Statistical analysis revealed that at 2 Gy survival of A549 cells was significantly higher ($p < 0.05$) than any of the other three cell lines. No other significant differences in survival following BB irradiation were seen between any of the cell lines, at any of the given doses. Having established that the cell lines under study displayed comparable sensitivity to BB irradiation we next evaluated MRT irradiation sensitivity, and predicted survival based upon the LQ-model with BB parameters (eq. (2)). Figure 3 shows the survival of the four cell lines following either BB or MRT, as well as the LQ-model based predicted survival
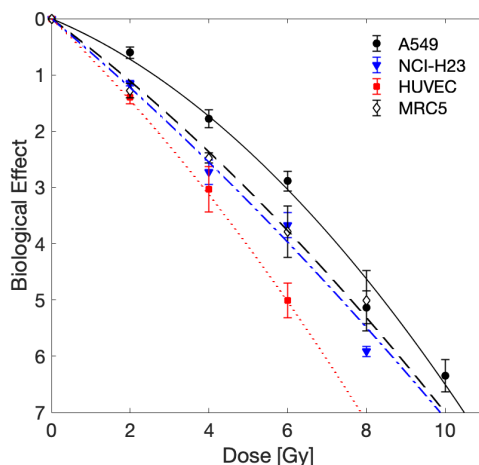
Figure 2. Biological effect of BB irradiation. Mean values and standard deviation of three independent experiments are shown. Data were fit by the LQ-model as indicated by lines (solid: A549, dashed: NCI-H23, dashed-dotted: MRC5, dotted: HUVEC); fit parameters obtained are shown in Table 1.

Cell line	$\alpha\ [Gy^{-1}]$	$\beta\ [Gy^{-2}]$
MRC5	0.52 ± 0.06	0.018 ± 0.007
NCI-H23	0.59 ± 0.07	0.012 ± 0.009
A549	0.29 ± 0.05	0.036 ± 0.006
HUVEC	0.67 ± 0.01	0.028 ± 0.002

Table 1: LQ-model parameters α and β for homogeneous BB irradiation with 95% confidence bounds.

with relevant uncertainty bands. For all cell lines BB irradiation was more effective than MRT when compared at equal integral dose levels. Additionally, all four cell lines tolerated MRT less than predicted by the LQ-model with BB parameters. However, the clonogenic survival observed for the normal cells (MRC-5 and HUVEC) after MRT was closer to their predicted survival than the survival observed for the tumour cell lines. In the case of the normal lung fibroblast cell line MRC-5 the observed survival fell within the uncertainties of the prediction at integral doses higher than 15 Gy.

To assess the importance of the spatial distribution of dose gradients for MRT on the survival of normal and tumour cells we performed dose mixing experiments, where cells were irradiated with BB irradiation at two dose levels and then the cells were mixed post irradiation with a PVDR of 22 and 80% of cells receiving valley dose. Figure 4 demonstrates a response similar to that of MRT, as measured by clonogenic survival, can be achieved in this way.

Figure 5 compares the clonogenic survival following BB irradiation and the valley dose (corrected to account for differences in seeding numbers) of the dose mixing experiments in order to evaluate differential response of normal and tumour cells in a direct comparison without model prediction. For all four cell lines the survival of the cell population receiving the mixing valley dose was below that of the BB irradiated cells. Importantly, this difference in survival is much more pronounced for the tumour cells than the normal cells. Whereas in the two normal cell lines the survival at the highest valley dose of 3.6 Gy falls within the margins of error of survival following BB irradiation (no significant difference), there was a significant difference for the A549 and NCI-H23 cells ($p < 0.01$, unpaired t-test).
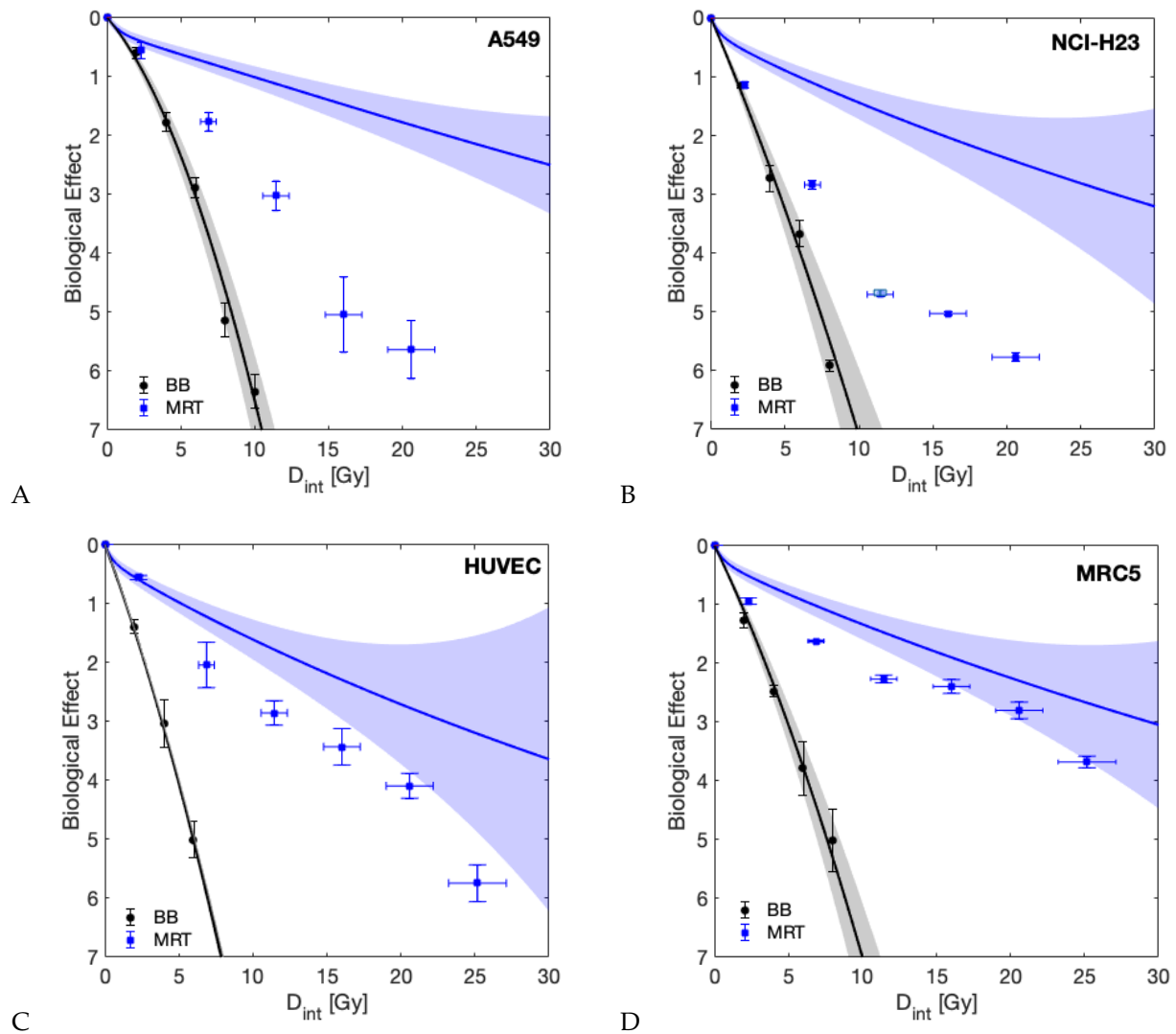
Figure 3. The biological effect of the investigated cell lines over integral dose (D_{int}) for BB and MRT together with the surviving fraction predicted by the LQ-model using BB parameters (solid lines). Shaded areas represent uncertainty due to LQ-model parameter fit uncertainty and dosimetric uncertainty as indicated in Figure 1. Data are shown for A) A549, B) NCI-H23 C) HUVEC and D) MRC-5 cells.
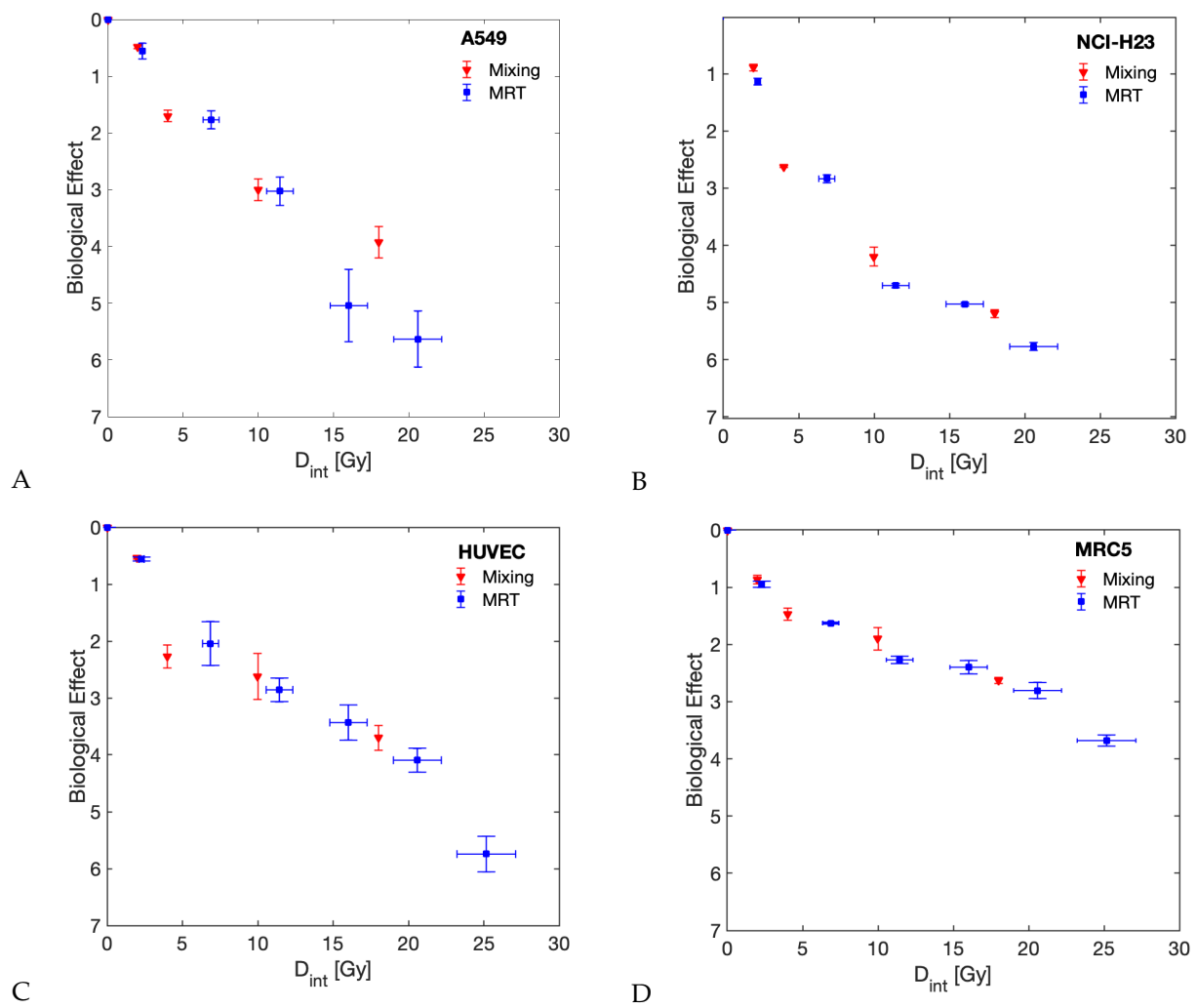
Figure 4. Comparing biological effect of MRT and dose mixing experiments as a function of integral dose. Survival curves are shown for A) A549, B) NCI-H23 C) HUVEC and D) MRC-5
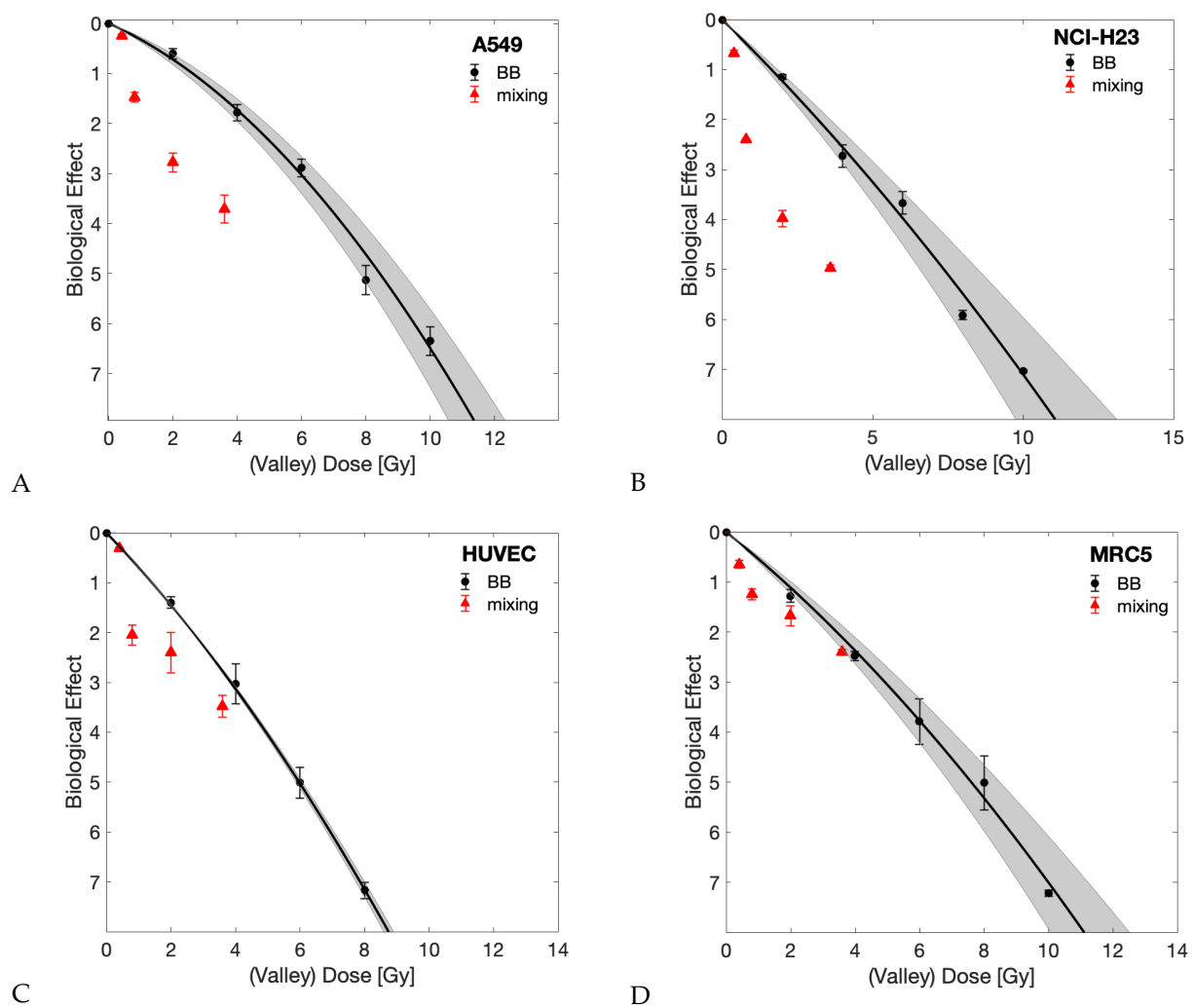
Figure 5. Comparing biological effect of BB against the valley dose of dose mixing experiment. Dose mixing surviving fractions were divided by 0.8 to account for only 80% of cells receiving the valley dose. BB results are shown with the relevant LQ-model fit (shaded areas indicate fit 95% confidence intervals). Survival curves are shown for A) A549, B) NCI-H23 C) HUVEC and D) MRC-5

4. Discussion

In this study we aimed to address three unmet research questions in the field of MRT: i) is there a differential response of normal and tumour cell lines to MRT in vitro? ii) can the cellular response observed after synchroton MRT be recapitulated using bench-top equipment and in the absence of FLASH effects and iii) how to best compare cell survival following BB irradiation to survival following exposure to inhomogeneous MRT dose distributions to obtain a biologically more meaningful representation compared to plotting as a function of either peak, valley or mean (i.e. integral) dose levels?

To date, there are few reports of a normal tissue sparing effects following spatially fractionated radiation at an *in vitro* level: whereas Ibahim et al. were unable to demonstrate normal tissue sparing [19], Peng et al. reported that the specific field patterns influenced the results and that 2.5 mm stripes but not 5 mm stripes resulted in decreased cell survival of tumour cell lines compared to homogeneous radiation [23]. Here, we demonstrated enhanced cell killing by MRT compared to BB (see Figure 3). This effect was significantly more pronounced in tumour cells compared to normal cells. As such, it indicates that the differential effect of MRT *in vitro* enhanced tumour cell killing rather than providing improved normal tissue sparing as suggested by multiple studies *in vivo* [2,9,10,32,33]. We suggest that bystander signalling between cells is responsible for the additional cell killing observed, as indicated by several previous analyses[34]. Tumour cells were markedly more sensitive to mixed beam irradiations than normal cells, particularly when considering they showed equivalent sensitivity to BB irradiation. One possible explanation is that the normal cell lines we used are less sensitive to bystander signalling than the tumour cell lines. It is well documented that not all cell lines are able to produce bystander signals [35,36] and are equally responsive to them. Specifically, both actively proliferating and transcriptionally active cells are more sensitive to bystander signals [37,38] which supports our observations of more actively proliferating tumour cells being more sensitive to MRT than normal cells exhibiting slower doubling times. Future experimental analysis should address the mechanisms underlying the cellular response to MRT or mixed dose irradiation to confirm this hypothesis.

It should be stressed that our results reflect clonogenic cell survival. Clonogenic assays are generally considered the gold-standard method for evaluation of radiosensitivity. For this assay cells are trypsinised following irradiation (removing them from the spatial pattern) and plated at a relatively low density ($\approx 5 - 1000 cells/cm^2$). In such a setting, cell-cell communication seems to be of importance after irradiation as a delayed event, as opposed to taking place during the radiation exposure itself. This would be in agreement with the accepted time frames of bystander signalling [39]. The spatial arrangement of the delivered dose was found here to be irrelevant for measured surviving fractions as the dose mixing experiments (Figure 4) demonstrate that the clonogenic survival following MRT can be replicated by separately irradiating cells with homogeneous peak or valley doses and mixing them post irradiation. This finding may be specific to the clonogenic assay and it is possible that results would differ for assays where the cells remain *in situ* after irradiation or are plated at higher density than that used for clonogenic assays.

To the best of our knowledge we are the first to examine the effect of MRT *in vitro* using a bench-top X-ray source. The dose rates used here ($< 0.2\ Gy/s$) fall well below the range of dose rates previously attributed to FLASH effects [40]. Previous work employed synchrotron sources[19,23,41,42] and therefore it has been impossible to distinguish if any differential effects of MRT and BB irradiation were due to the spatial fractionation, or a result of FLASH effects. Here, we can discount any involvement of FLASH effects and attribute the differential response of normal and tumour cells wholly to the irradiation with high (peak) and low (valley) doses, either in the form of MRT or by post-mixing of separate BB irradiations. A similar conclusion was made by Smyth *et al.* who compared the relative toxicity of MRT and BB radiation at high and low dose rates [25]. They saw no evidence of normal tissue sparing following BB irradiation at dose rates of 37 to 41

241 Gy/s which could be considered marginally below the range of dose rates typically
242 associated with FLASH effects.
243 The work presented further contributes to the ongoing discussion of whether it is appro-
244 priate to compare valley, peak or mean dose of MRT to BB doses. Whilst it is generally
245 accepted that the peak dose is not the main contributor to cellular response to MRT,
246 there remains evidence that neither integral nor valley dose [19] can accurately predict
247 cellular response to MRT. Given the linear quadratic dose relation of cell survival, MRT
248 is expected to yield higher survival relative to BB at the same integral dose levels (as also
249 observed in Figure 3). Valley dose on the other hand yields lower surviving fractions for
250 MRT compared to BB since cells exposed to peak doses are unlikely to form colonies.
251 We hence included model predictions into the visualisation of our results (Figure 3) that
252 account for the full dose-spectrum delivered to be able to compare BB and MRT directly.
253 Additionally, through dose mixing experiments, with known fractions of cells receiving
254 only peak or valley doses, we were able to directly compare BB and spatially fractionated
255 RT cell survival as a function of valley dose (with appropriate correction to account for
256 only 80% of cells receiving this dose). The results obtained from these two approaches
257 agreed and demonstrate an increased tumour cell killing in the presence of ablated cells.
258 This implies that valley dose is not the only factor contributing to cell survival but that
259 ablated cells negatively impact the survival of the population receiving the valley dose
260 by bystander signalling.

261 **5. Conclusions**

262 Using a bench-top x-ray source we have demonstrated a differential *in vitro* response
263 of lung cancer cell lines, endothelial cells and fibroblasts to microbeam irradiation at
264 dose rates precluding the presence of FLASH effects. Specifically, we observed an
265 increased tumour cell sensitivity to MRT, whereas normal cell survival following MRT
266 was comparable to survival after BB irradiation. Cell survival after MRT was replicated
267 by mixing populations of cells irradiated separately with high and low BB doses. Both
268 of these results indicate a role for bystander signalling in the response of both, normal
269 and tumour cells to MRT *in vitro*.

Abbreviations

The following abbreviations are used in this manuscript:

DVH	Dose rate volume histogram
RT	Radiation therapy
MRT	Microbeam radiation therapy
BB	Broad beam
OAR	Organ at risk
PVDR	Peak-to-valley dose ratio
LQ model	Linear quadratic model

Appendix A. Tabulated cell survival data

Table 1: Broad beam cell survival data for the four cell lines used. Mean values and standard deviations of three independent repeat experiments are reported.

Dose [Gy]	HUVEC	MRC5	NCI-H23	A549
0	1 ± 0	1 ± 0	1 ± 0	1 ± 0
2	0.25 ± 0.03	0.28 ± 0.04	0.32 ± 0.02	0.55 ± 0.06
4	0.048 ± 0.019	0.084 ± 0.008	0.065 ± 0.014	0.17 ± 0.03
6	0.007 ± 0.002	0.023 ± 0.01	0.026 ± 0.006	0.056 ± 0.01
8	0.001 ± 0.0001	0.007 ± 0.004	0.003 ± 0.0002	0.006 ± 0.002
10		0.001 ± 0.00005	0.001 ± 0.00002	0.002 ± 0.001

Table 2: Microbeam cell survival data for the four cell lines used. Mean values and standard deviations of three independent repeat experiments are reported.

Mean Dose [Gy]	HUVEC	MRC5	NCI-H23	A549
0	1 ± 0	0.5 ± 0.25	1 ± 0	1 ± 0
2	0.57 ± 0.02	0.3 ± 0.14	0.32 ± 0.02	0.57 ± 0.08
6	0.13 ± 0.05	0.09 ± 0.02	0.059 ± 0.004	0.17 ± 0.03
10	0.06 ± 0.01	0.035 ± 0.011	0.009 ± 0.0004	0.049 ± 0.012
14	0.03 ± 0.01	0.021 ± 0.006	0.007 ± 0.0002	0.006 ± 0.004
18	0.017 ± 0.004	0.01 ± 0.003	0.003 ± 0.0002	0.004 ± 0.002
22	0.003 ± 0.001	0.002 ± 0.001		
26	0.001 ± 0.0006	0.001 ± 0.0001		

Table 3: Mixed broad beam cell survival data for the four cell lines used. Mean values and standard deviations of three independent repeat experiments are reported.

Mean Dose [Gy]	HUVEC	MRC5	NCI-H23	A549
0	1 ± 0	1 ± 0	1 ± 0	1 ± 0
2	0.59 ± 0.01	0.42 ± 0.03	0.41 ± 0.02	0.62 ± 0.02
4	0.1 ± 0.02	0.23 ± 0.024	0.073 ± 0.001	0.18 ± 0.02
10	0.072 ± 0.029	0.15 ± 0.029	0.015 ± 0.002	0.05 ± 0.009
18	0.025 ± 0.005	0.072 ± 0.004	0.006 ± 0.0004	0.02 ± 0.005

References

1. Slatkin, D.N.; Spanne, P.; Dilmanian, F.; Sandborg, M. Microbeam radiation therapy. *Medical physics* **1992**, *19*, 1395–1400.
2. Slatkin, D.; Spanne, P.; Dilmanian, F.; Gebbers, J.; Laissue, J. Subacute neuropathological effects of microplanar beams of x-rays from a synchrotron wiggler. *Proceedings of the National Academy of Sciences* **1995**, *92*, 8783–8787.
3. Dilmanian, F.; Morris, G.; Le, G.D.; Huang, X.; Ren, B.; Bacarian, T.; Allen, J.; Kalef-Ezra, J.; Orion, I.; Rosen, E.; others. Response of avian embryonic brain to spatially segmented x-ray microbeams. *Cellular and molecular biology (Noisy-le-Grand, France)* **2001**, *47*, 485–493.
4. Laissue, J.A.; Bartzsch, S.; Blattmann, H.; Bräuer-Krisch, E.; Bravin, A.; Dalléry, D.; Djonov, V.; Hanson, A.L.; Hopewell, J.W.; Kaser-Hotz, B.; others. Response of the rat spinal cord to X-ray microbeams. *Radiotherapy and oncology* **2013**, *106*, 106–111.

5.   Bouchet, A.; Serduc, R.; Laissue, J.A.; Djonov, V. Effects of microbeam radiation therapy on normal and tumoral blood vessels. *Physica Medica: European Journal of Medical Physics* **2015**, *31*, 634–641.

6.   Serduc, R.; Van de Looij, Y.; Francony, G.; Verdonck, O.; Van Der Sanden, B.; Laissue, J.; Farion, R.; Bräuer-Krisch, E.; Siegbahn, E.A.; Bravin, A.; others. Characterization and quantification of cerebral edema induced by synchrotron x-ray microbeam radiation therapy. *Physics in Medicine & Biology* **2008**, *53*, 1153.

7.   Laissue, J.A.; Blattmann, H.; Di Michiel, M.; Slatkin, D.N.; Lyubimova, N.; Guzman, R.; Zimmermann, W.; Birrer, S.; Bley, T.; Kircher, P.; others. Weanling piglet cerebellum: a surrogate for tolerance to MRT (microbeam radiation therapy) in pediatric neuro-oncology. Penetrating Radiation Systems and Applications III. International Society for Optics and Photonics, 2001, Vol. 4508, pp. 65–74.

8.   Potez, M.; Bouchet, A.; Wagner, J.; Donzelli, M.; Bräuer-Krisch, E.; Hopewell, J.W.; Laissue, J.; Djonov, V. Effects of Synchrotron X-Ray Micro-beam Irradiation on Normal Mouse Ear Pinnae. *International Journal of Radiation Oncology*Biology*Physics* **2018**, *101*, 680–689. doi:https://doi.org/10.1016/j.ijrobp.2018.02.007.

9.   Laissue, J.A.; Geiser, G.; Spanne, P.O.; Dilmanian, F.A.; Gebbers, J.O.; Geiser, M.; Wu, X.Y.; Makar, M.S.; Micca, P.L.; Nawrocky, M.M.; others. Neuropathology of ablation of rat gliosarcomas and contiguous brain tissues using a microplanar beam of synchrotron-wiggler-generated X rays. *International journal of cancer* **1998**, *78*, 654–660.

10.   Bräuer-Krisch, E.; Serduc, R.; Siegbahn, E.; Le Duc, G.; Prezado, Y.; Bravin, A.; Blattmann, H.; Laissue, J. Effects of pulsed, spatially fractionated, microscopic synchrotron X-ray beams on normal and tumoral brain tissue. *Mutation Research/Reviews in Mutation Research* **2010**, *704*, 160–166.

11.   Regnard, P.; Le Duc, G.; Bräuer-Krisch, E.; Tropres, I.; Siegbahn, E.A.; Kusak, A.; Clair, C.; Bernard, H.; Dallery, D.; Laissue, J.A.; others. Irradiation of intracerebral 9L gliosarcoma by a single array of microplanar x-ray beams from a synchrotron: balance between curing and sparing. *Physics in Medicine & Biology* **2008**, *53*, 861.

12.   Bouchet, A.; Lemasson, B.; Le Duc, G.; Maisin, C.; Bräuer-Krisch, E.; Siegbahn, E.A.; Renaud, L.; Khalil, E.; Rémy, C.; Poillot, C.; others. Preferential effect of synchrotron microbeam radiation therapy on intracerebral 9L gliosarcoma vascular networks. *International Journal of Radiation Oncology• Biology• Physics* **2010**, *78*, 1503–1512.

13.   Yuan, H.; Zhang, L.; Frank, J.E.; Inscoe, C.R.; Burk, L.M.; Hadsell, M.; Lee, Y.Z.; Lu, J.; Chang, S.; Zhou, O. Treating Brain Tumor with Microbeam Radiation Generated by a Compact Carbon-Nanotube-Based Irradiator: Initial Radiation Efficacy Study. *Radiation Research* **2015**, *184*, 322 – 333. doi:10.1667/RR13919.1.

14.   Potez, M.; Fernandez-Palomo, C.; Bouchet, A.; Trappetti, V.; Donzelli, M.; Krisch, M.; Laissue, J.; Volarevic, V.; Djonov, V. Synchrotron Microbeam Radiation Therapy as a New Approach for the Treatment of Radioresistant Melanoma: Potential Underlying Mechanisms. *International Journal of Radiation Oncology*Biology*Physics* **2019**, *105*, 1126–1136. doi:https://doi.org/10.1016/j.ijrobp.2019.08.027.

15.   Sabatasso, S.; Laissue, J.A.; Hlushchuk, R.; Graber, W.; Bravin, A.; Bräuer-Krisch, E.; Corde, S.; Blattmann, H.; Gruber, G.; Djonov, V. Microbeam radiation-induced tissue damage depends on the stage of vascular maturation. *International Journal of Radiation Oncology• Biology• Physics* **2011**, *80*, 1522–1532.

16.   Blattmann, H.; Gebbers, J.O.; Bräuer-Krisch, E.; Bravin, A.; Le Duc, G.; Burkard, W.; Di Michiel, M.; Djonov, V.; Slatkin, D.; Stepanek, J.; others. Applications of synchrotron X-rays to radiotherapy. *Nuclear Instruments and Methods in Physics Research Section A: Accelerators, Spectrometers, Detectors and Associated Equipment* **2005**, *548*, 17–22.

17.   Van Der Sanden, B.; Bräuer-Krisch, E.; Siegbahn, E.A.; Ricard, C.; Vial, J.C.; Laissue, J. Tolerance of arteries to microplanar X-ray beams. *International Journal of Radiation Oncology• Biology• Physics* **2010**, *77*, 1545–1552.

18.   Bouchet, A.; Sakakini, N.; El Atifi, M.; Le Clec'h, C.; Brauer, E.; Moisan, A.; Deman, P.; Rihet, P.; Le Duc, G.; Pelletier, L. Early gene expression analysis in 9L orthotopic tumor-bearing rats identifies immune modulation in molecular response to synchrotron microbeam radiation therapy. *PLoS One* **2013**, *8*, e81874.

19.   Ibahim, M.; Yang, Y.; Crosbie, J.; Stevenson, A.; Cann, L.; Paiva, P.; Rogers, P. Eosinophil-associated gene pathways but not eosinophil numbers are differentially regulated between synchrotron microbeam radiation treatment and synchrotron broad-beam treatment by 48 hours postirradiation. *Radiation research* **2015**, *185*, 60–68.

20.   Yang, Y.; Crosbie, J.C.; Paiva, P.; Ibahim, M.; Stevenson, A.; Rogers, P.A. In vitro study of genes and molecular pathways differentially regulated by synchrotron microbeam radiotherapy. *Radiation research* **2014**, *182*, 626–639.

21.   Smilowitz, H.; Blattmann, H.; Bräuer-Krisch, E.; Bravin, A.; Di Michiel, M.; Gebbers, J.O.; Hanson, A.; Lyubimova, N.; Slatkin, D.; Stepanek, J.; others. Synergy of gene-mediated immunoprophylaxis and microbeam radiation therapy for advanced intracerebral rat 9L gliosarcomas. *Journal of neuro-oncology* **2006**, *78*, 135–143.

22.   Asur, R.S.; Sharma, S.; Chang, C.W.; Penagaricano, J.; Kommuru, I.M.; Moros, E.G.; Corry, P.M.; Griffin, R.J. Spatially fractionated radiation induces cytotoxicity and changes in gene expression in bystander and radiation adjacent murine carcinoma cells. *Radiation research* **2012**, *177*, 751–765.

23.   Peng, V.; Suchowerska, N.; Rogers, L.; Claridge Mackonis, E.; Oakes, S.; McKenzie, D.R. Grid therapy using high definition multileaf collimators: realizing benefits of the bystander effect. *Acta Oncologica* **2017**, *56*, 1048–1059.

24.   Wilson, J.D.; Hammond, E.M.; Higgins, G.S.; Petersson, K. Ultra-High Dose Rate (FLASH) Radiotherapy: Silver Bullet or Fool's Gold? *Frontiers in Oncology* **2020**, *9*. doi:10.3389/fonc.2019.01563.

25. Smyth, L.M.; Donoghue, J.F.; Ventura, J.A.; Livingstone, J.; Bailey, T.; Day, L.R.; Crosbie, J.C.; Rogers, P.A. Comparative toxicity of synchrotron and conventional radiation therapy based on total and partial body irradiation in a murine model. *Scientific reports* **2018**, *8*, 12044.

26. Ibahim, M.J.; Crosbie, J.C.; Yang, Y.; Zaitseva, M.; Stevenson, A.W.; Rogers, P.A.; Paiva, P. An evaluation of dose equivalence between synchrotron microbeam radiation therapy and conventional broadbeam radiation using clonogenic and cell impedance assays. *PLoS One* **2014**, *9*, e100547.

27. Bromley, R.; Oliver, L.; Davey, R.; Harvie, R.; Baldock, C. Predicting the clonogenic survival of A549 cells after modulated x-ray irradiation using the linear quadratic model. *Physics in Medicine & Biology* **2008**, *54*, 187.

28. Burger, K.; Ilicic, K.; Dierolf, M.; Gﬓnther, B.; Walsh, D.W.M.; Schmid, E.; Eggl, E.; Achterhold, K.; Gleich, B.; Combs, S.E.; Molls, M.; Schmid, T.E.; Pfeiffer, F.; Wilkens, J.J. Increased cell survival and cytogenetic integrity by spatial dose redistribution at a compact synchrotron X-ray source. *PLOS ONE* **2017**, *12*, 1–15. doi:10.1371/journal.pone.0186005.

29. Bartzsch, S.; Cummings, C.; Eismann, S.; Oelfke, U. A preclinical microbeam facility with a conventional x-ray tube. *Medical physics* **2016**, *43*, 6301–6308.

30. Bartzsch, S.; Lott, J.; Welsch, K.; Bräuer-Krisch, E.; Oelfke, U. Micrometer-resolved film dosimetry using a microscope in microbeam radiation therapy. *Medical physics* **2015**, *42*, 4069–4079.

31. Fowler, J.F. The linear-quadratic formula and progress in fractionated radiotherapy. *The British journal of radiology* **1989**, *62*, 679–694.

32. Fernandez-Palomo, C.; Trappetti, V.; Potez, M.; Pellicioli, P.; Krisch, M.; Laissue, J.; Djonov, V. Complete Remission of Mouse Melanoma after Temporally Fractionated Microbeam Radiotherapy. *Cancers* **2020**, *12*. doi:10.3390/cancers12092656.

33. Dilmanian, F.A.; Morris, G.M.; Zhong, N.; Bacarian, T.; Hainfeld, J.F.; Kalef-Ezra, J.; Brewington, L.J.; Tammam, J.; Rosen, E.M. Murine EMT-6 Carcinoma: High Therapeutic Efficacy of Microbeam Radiation Therapy. *Radiation Research* **2003**, *159*, 632 – 641. doi:10.1667/0033-7587(2003)159[0632:MECHTE]2.0.CO;2.

34. Mothersill, C.; Rusin, A.; Fernandez-Palomo, C.; Seymour, C. History of bystander effects research 1905-present; what is in a name? *International Journal of Radiation Biology* **2018**, *94*, 696–707. doi:10.1080/09553002.2017.1398436.

35. Mothersill, C.; Seymour, C. Radiation-induced bystander effects: past history and future directions. *Radiation research* **2001**, *155*, 759–767.

36. Mukherjee, S.; Chakraborty, A. Radiation-induced bystander phenomenon: insight and implications in radiotherapy. *International Journal of Radiation Biology* **2019**, *95*, 243–263. doi:10.1080/09553002.2019.1547440.

37. Dickey, J.S.; Baird, B.J.; Redon, C.E.; Avdoshina, V.; Palchik, G.; Wu, J.; Kondratyev, A.; Bonner, W.M.; Martin, O.A. Susceptibility to bystander DNA damage is influenced by replication and transcriptional activity. *Nucleic acids research* **2012**, *40*, 10274–10286.

38. Megha Anilkumar, K.; Safa Abdul, S.B.; Sidonia Vallas, X.; Murugan, A.; Thayalan, K.; Perumal, V. Direct and Bystander Effect on Cervix Cancer Cells (SiHa) Exposed to High Dose-Rate Gamma Radiation Sourced from Ir 192 Used in Brachytherapy. *International Journal of Radiology and Radiation Oncology* **2015**, *1*, 007–013. doi:10.17352/ijrro.000004.

39. Prise, K.M.; O'Sullivan, J.M. Radiation-induced bystander signalling in cancer therapy. *Nature Reviews Cancer* **2009**, *9*, 351–360. doi:10.1038/nrc2603.

40. Favaudon, V.; Fouillade, C.; Vozenin, M. Ultrahigh dose-rate," flash" irradiation minimizes the side-effects of radiotherapy. *Cancer radiotherapie: journal de la Societe francaise de radiotherapie oncologique* **2015**, *19*, 526–531.

41. Schültke, E.; Fiedler, S.; Menk, R.H.; Jaekel, F.; Dreossi, D.; Casarin, K.; Tromba, G.; Bartzsch, S.; Kriesen, S.; Hildebrandt, G.; Arfelli, F. Perspectives for microbeam irradiation at the SYRMEP beamline. *Journal of Synchrotron Radiation* **2021**, *28*, 410–418. doi:10.1107/S1600577521000400.

42. Engels, E.; Li, N.; Davis, J.; Paino, J.; Cameron, M.; Dipuglia, A.; Vogel, S.; Valceski, M.; Khochaiche, A.; O'Keefe, A.; Barnes, M.; Cullen, A.; Stevenson, A.; Guatelli, S.; Rosenfeld, A.; Lerch, M.; Corde, S.; Tehei, M. Toward personalized synchrotron microbeam radiation therapy. *Scientific Reports* **2020**, *10*, 8833. doi:10.1038/s41598-020-65729-z.